



Physicochemical analysis of liposome membranes consisting of model lipids in the stratum corneum

Kenichi Aburai, Saeko Yoshino, Kenichi Sakai, Hideki Sakai, Masahiko Abe, Nicolas Loiseau, Walter Holleran, Yoshikazu Uchida, Kazutami Sakamoto

► To cite this version:

Kenichi Aburai, Saeko Yoshino, Kenichi Sakai, Hideki Sakai, Masahiko Abe, et al.. Physicochemical analysis of liposome membranes consisting of model lipids in the stratum corneum. *Journal of oleo science*, 2011, 60 (4), pp.197-202. hal-02647131

HAL Id: hal-02647131

<https://hal.inrae.fr/hal-02647131>

Submitted on 29 May 2020

HAL is a multi-disciplinary open access archive for the deposit and dissemination of scientific research documents, whether they are published or not. The documents may come from teaching and research institutions in France or abroad, or from public or private research centers.

L'archive ouverte pluridisciplinaire **HAL**, est destinée au dépôt et à la diffusion de documents scientifiques de niveau recherche, publiés ou non, émanant des établissements d'enseignement et de recherche français ou étrangers, des laboratoires publics ou privés.

Physicochemical Analysis of Liposome Membranes Consisting of Model Lipids in the Stratum Corneum

Kenichi Aburai^{1*}, Saeko Yoshino¹, Kenichi Sakai¹, Hideki Sakai¹, Masahiko Abe¹, Nicolas Loiseau², Walter Holleran², Yoshikazu Uchida² and Kazutami Sakamoto^{1,3}

¹ Department of Pure and Applied Chemistry, Tokyo University of Science (2641 Yamazaki, Noda, Chiba, 278-8510, JAPAN)

² Department of Dermatology, University of California San Francisco (4150 Clement Street, San Francisco, CA94121-1545, USA)

³ Faculty of Pharmacy, Chiba Institute of Science (15-8 Shiomi, Choshi, Chiba, 288-0025, JAPAN)

Abstract: Lamellar lipid layers in the stratum corneum (SC), the outermost layer of the skin, act as a primary permeability barrier to protect the body. The roles of SC lipid composition and membrane structure in skin barrier function have been extensively investigated using ex-vivo SC samples and reconstructed SC lipids in the form of multi-lamellar lipids or liposomes. The primary lipids, especially ceramide, have been found to be highly important. Atopic dermatitis (AD) is a well-known chronic inflammatory skin disease with immunologic and epidermal abnormalities of the permeability barrier; therefore, a comparison of SC lipids in AD skin with those in normal skin is a promising method to explore the mechanisms of skin barrier function. Here, we focused on the effect of sphingoids (ceramide metabolites and a minor component of the SC lipids) and their content/species on skin barrier function. A significant difference in the leakage ratio was observed between model SC lipid liposomes with a different sphingolipid ratio (sphingosine/sphinganine), with a value of 5.43 for normal skin vs. 14.3 for AD skin. This result shows a good concordance with AD mouse experiments. Therefore, an alteration in the composition of minor SC lipids resulting from a ceramide metabolic abnormality can affect the membrane integrity (i.e., skin barrier function). Small angle X-ray scattering (SAXS) measurements revealed no distinct differences in the SAXS pattern between the 3 models, with all models forming a rigid membrane (i.e., a nearly hydrated solid). According to increasing the temperature, the peaks indicated that the lamellar structures decreased in all models and that the lateral packing of lipids decreased, which suggested annealing or melting of the gel to a liquid crystal, although no distinct phase transition was observed through fluorescence anisotropy measurements. Hence, we assume that the altered sphingoid composition triggers local membrane structural changes (i.e., formation of domains or clusters).

Key words: stratum corneum (SC), atopic dermatitis (AD), sphingolipid, permeability, skin barrier, membrane property

1 INTRODUCTION

The stratum corneum (SC) is located in the outermost layer of the skin and mainly comprises corneocytes (cells) and intercellular lipids. The SC intercellular lipids (SC lipids) consist primarily of ceramides, long-chain fatty acids, and cholesterol (Chol). SC lipids form lamellar membranes that serve as the primary permeability barrier for protecting the skin against both excess water loss and penetration by foreign substances¹⁻³. Although SC lipids have basic bilayer structures similar to general biomembranes, there are two fundamental differences between them. First, general biomembranes are in a lyotropic liquid crystal phase under viable conditions so that lipids, mainly composed of phos-

pholipids, are soft and mobile, whereas SC lipids are in a gel phase that is well structured and exhibits rigid packing. Second, there are morphological differences. Biomembranes are uni-lamellar bilayers enclosed by an extracellular matrix, whereas SC lipids are flat, multi-lamellar layers stacked between corneocytes. The roles of SC lipid composition and membrane structure in skin barrier function have been extensively investigated. Although it has been suggested that the role of major lipids (especially ceramides) is highly important⁴⁻⁸, the key mechanisms governing skin barrier function are still unresolved.

Atopic dermatitis (AD) is a well-known chronic inflammatory skin disease with immunological and epidermal abnor-

*Correspondence to: Kenichi Aburai, Department of Pure and Applied Chemistry, Tokyo University of Science, 2641 Yamazaki, Noda, Chiba, 278-8510, JAPAN

E-mail: j7208702@ed.noda.tus.ac.jp, kasakamoto@cis.ac.jp

Accepted November 17, 2010 (received for review October 12, 2010)

Journal of Oleo Science ISSN 1345-8957 print / ISSN 1347-3352 online

<http://www.jstage.jst.go.jp/browse/jos/>

malities in the permeability barrier in conjunction with alterations in the barrier lipid profiles, including ceramide^{9,10}. Thus, AD is a suitable model to investigate the relationship between structure and function in epidermal permeability. Although previous studies have shown deficiencies in the specific ceramide species ceramide 1 and ceramide 3, as well as altered epidermal ceramide metabolism^{11–13}, the roles of the ceramide metabolites sphingosine (So) and sphinganine (Sa) remain unknown.

Because of the amphiphilic properties of sphingoid bases, we have hypothesized that sphingoid bases modulate SC membrane barrier permeability and stability and that changes in sphingoid base levels affect epidermal permeability barrier function in the SC. In previous studies, we assessed epidermal lipid content in both normal and AD mouse models^{14, 15}. Similar to human AD, decreases in ceramide 1 and ceramide 3 were evident in the AD mouse model. Therefore, we further investigated the sphingoid base levels. Sphingosine (d18:1, So) and sphinganine (d18:0, Sa) were the major SC sphingoid base species (>95% of total sphingoid bases) in both normal and AD mice. Meanwhile, the total sphingoid base content increased 1.5-fold in the SC of AD mice. Significantly, the So-to-Sa ratio markedly increased from 5.43 to 14.3 in the SC of AD mice. Moreover, we assessed the effects of sphingoid bases on membrane permeability using liposomes comprising Chol, ceramides, and free fatty acids, mimicking either normal or AD mouse models by means of surfactant perturbation with sodium lauryl sulfate. These studies revealed that an increase in membrane permeability resulted from an alteration in the So-to-Sa ratio¹⁵.

In this study, we investigated the spontaneous leakage rate of an encapsulated fluorescence probe in model liposomes. We further examined the physicochemical roles of sphingoid bases in the structure and function of hydrated SC lipids in conjunction with permeability barrier function by using small-angle X-ray scattering (SAXS) and fluorescent anisotropy analyses. Our results suggest that the altered lipid composition triggers local membrane structural changes (i.e., formation of domains or clusters) that produce permeability deficiencies in AD SC lipids.

2 EXPERIMENTAL PROCEDURES

2.1 Materials

The lipids N-octadecanoyl-D-erythro-sphingosine (ceramide 2, Cer 2, 98% pure), D-erythro-sphingosine (So, 98% pure), D-erythro-sphinganine (Sa, 98% pure; these 3 lipids were purchased from MATREYA LLC., Pennsylvania, USA), palmitic acid (PA, 95% pure; TCI Co. Ltd., Tokyo, Japan), and Chol (99% pure; Wako Pure Chemical Ind., Ltd., Osaka, Japan), were used for the preparation of liposomes (Fig. 1). Piperazine-1,4-bis(2-ethanesulfonic acid) (PIPES, DOJIN-DO Laboratory, Kumamoto, Japan) and 5N NaOH solution were used for the preparation of 20 mM pH 7.43 PIPES buffer. Phosphate-buffered saline (PBS; Wako Pure Chemical Ind., Ltd., Osaka, Japan) was used as a solvent. Rhodamine B (Rho, 98% pure; Kanto Chemical Co. Inc., Tokyo, Japan) was used as fluorescence probe to examine the leakage ratio from the liposomes. 1,6-Diphenyl-1,3,5-hexatriene (DPH) and tetrahydrofuran (THF, 99.5% pure), purchased from Wako Pure Chemical Ind. Ltd., Osaka, Japan, were used for fluorescence anisotropy measurements.

2.2 Preparation of liposomes

Three skin models (Table 1) were established previously¹⁵ and used for all experiments. All liposomes were prepared by probe sonication methods^{16, 17}. Each lipid was dissolved in chloroform to prepare 10 mM solutions. These solutions were added to a vial to meet each molar ratio. The majority of solvent was evaporated from the vial under N₂ gas. To remove the residual solvent, the vial was placed in vacuo for 16 h in the dark. PIPES buffer was added to

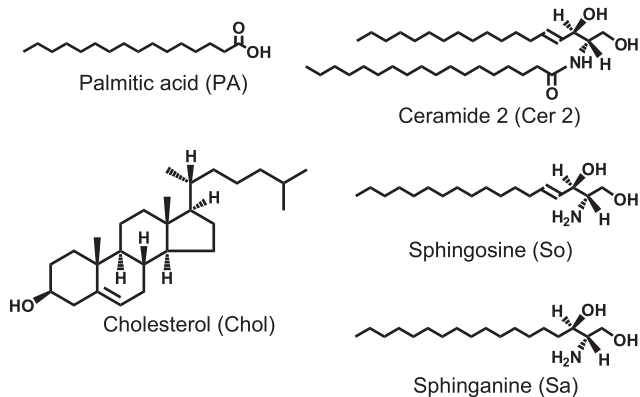


Fig. 1 Chemical structures of lipids

Table 1 Lipid components of model liposome

	Lipid components (molar ratio)					
	Cer 2	Chol	PA	So	Sa	So/Sa
NS (Normal skin model)	11.9	33.0	50.6	3.80	0.700	5.43
AS (Abnormal skin model)	11.7	32.4	49.8	5.70	0.400	14.3
3M (3 components)	12.5	34.5	53.0	—	—	—

the lipid film to a final adjusted concentration of 10 mM. The solution was then warmed at 80°C and vortexed for 3 min. The suspension was sonicated using a homogenizer (US-300T; Nihonseiki Kaisha Ltd., Tokyo, Japan) for 30 s and cooled with ice for 30 s. This process was carried out 10 times, and a liposomal suspension was obtained.

2.3 Transmission electron microscopic observations of liposomes

The liposomal suspension was frozen quickly in liquid propane using a cryopreparation chamber (Leica EM CPC; Leica Co., Tokyo, Japan). The frozen sample was transferred to a freeze fracture device (FR-7000A; Hitachi High-Technologies Co., Tokyo, Japan) and was fractured at −150°C. Platinum was deposited onto the fractured surface at an angle of 45°C, and carbon was evaporated at an angle of 90°C. The replica was recovered onto a copper 400-mesh grid after washing with acetone and water and observed under a transmission electron microscope (H-7650; Hitachi High-Technologies Co., Tokyo, Japan). As shown in Fig. 2, the formation of liposomes was observed for all model lipids.

2.4 Liposome leakage ratio measurements

To determine the liposome leakage ratio, liposomes containing Rho (Rho-liposomes) were prepared. Five mg/mL of Rho solution in PIPES buffer was added to a lipid thin film. After the liposomes were prepared, the mixtures were separated into Rho-liposomes and free Rho through a gel filtration column (Sephacrose™ CL-4B; GL Sciences Inc., To-

kyo, Japan). Rho-liposomes (200 µL) were placed in a dialysis membrane (UC-8-32-25; Viskase Co. Ltd., Chicago, USA) and set in 20 mL of PBS at 25, 40, and 60°C for 48 h. During an optional time, 500 µL of the membrane outer solution was collected and added to 200 µL of 10% Triton X-100 (Sigma-Aldrich Co., Missouri, USA) and 300 µL of PBS. The amount of leaked Rho contained in the 1 mL of outer solution samples was analyzed using a fluorescence spectrometer (RF5300PC; SHIMADZU Co., Kyoto, Japan). To calculate the leakage ratio, 20 µL of the Rho-liposome fractionated just after gel filtration (0 min) was analyzed. The leakage ratio was calculated by the following equation:

$$L = \frac{I_t}{I_0} \times 100 \quad (1)$$

where L is the leakage ratio, I_t is the Rho fluorescence intensity at an optional time, and I_0 is the Rho fluorescence intensity at 0 min (after gel filtration).

2.5 Small-angle X-ray scattering measurements

A SAXS experiment was carried out using a SAXSess camera (Anton-Paar Co. Ltd., Graz, Austria) and a PW3830 X-ray generator (PANalytical Ltd., ALMELO, Netherlands; operational at 40 kV and 50 mA). Each sample was filled into a thin quartz capillary and set in a sample holder unit (TCS120; Anton Paar Co. Ltd., Graz, Austria) at several temperatures for 1 h before the measurement. An imaging plate was used to record the scattering data and was read out by a Cyclone storage phosphor system (Perkin-Elmer Co. Ltd., Massachusetts, USA) to acquire a scattering pattern.

2.6 Fluorescence anisotropy measurements

Liposomes were labeled with DPH by adding 10 µL of 10 mM DPH/THF solution to 1 mL of liposomal suspension and then incubated at 37°C for 2 h in the dark. Measurements of fluorescence anisotropy were performed with a fluorescence spectrometer (Ex = 351 nm, Em = 430 nm). The fluorescence anisotropy was calculated by using the following equation:

$$A = \frac{I_0 - G \times I_{90}}{I_0 + 2G \times I_{90}} \quad (2)$$

where A is anisotropy, I_0 and I_{90} are the intensity measured in direction parallel and to polarized exciting light, and G is the instrumental constant.

3 RESULTS AND DISCUSSION

3.1 Leakage assay

In order to clarify the effects of sphingoid content and species on SC lipids and hence on skin permeability barrier function, we assessed the permeability of fluorescent probes encapsulated into liposomes with model SC lipid compositions. The model lipid compositions (Table 1) are

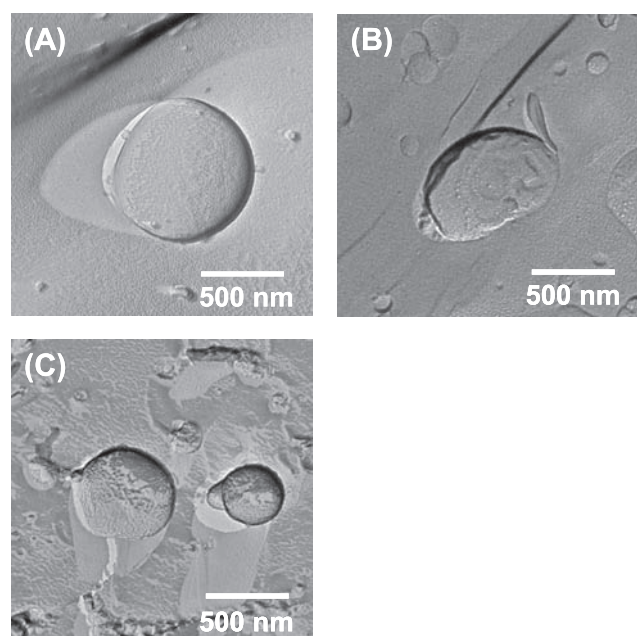


Fig. 2 FF-TEM images of liposomal suspensions. (A) NS, (B) AS, (C) 3M. Lipid concentration was fixed at 10 mM for the samples.

based on the analytical data for ceramide metabolites in mouse AD skin and normal skin¹⁵. As shown in **Table 1**, the basic composition of Cer 2/Chol/PA is 12.5/34.5/53 for 3M, which is free of sphingoid. The normal skin model (NS) and abnormal skin model (AS) are model lipids based on 3M but with sphingoids as partial metabolites of ceramide in the SC. For NS and AS, the amount of sphingoids are comparable to each other at 4.5 and 6.1 mol%, respectively. On the other hand, the ratio of sphingoid, namely So to Sa, increased from 5.43 (NS) to 14.3 (AS). Such slight differences in sphingoid content/species are likely to contribute to the barrier defects in AD skin¹⁵.

Figure 3 shows the leakage ratio of Rho from liposomes at 3 h. While the leakage ratio of NS and 3M were comparable, the leakage of Rho from AS was significantly higher than that from NS, indicating a barrier function deficiency in the AD mouse from which these compositions were determined. Because sphingoid lipids are a minor component of the SC lipids, it is noteworthy that a difference in the So/Sa ratio (i.e., 5.43 for NS vs. 14.3 for AS) leads to permeability differences between the 3 models.

Figure 3 shows the effect of temperature on the leakage ratio for the model lipids. In parallel with the increase in temperature, the leakage ratio increased linearly in all skin models, but AS was more strongly dependent on the tem-

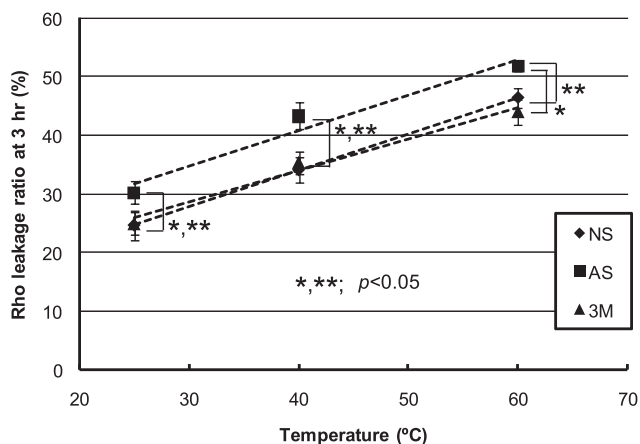


Fig. 3 Correlation between leakage ratio and temperature. Horizontal axes shows a temperature and longitudinal axes shows a leakage ratio at 3 h after gel filtration. Significant difference (*; 3M v.s. AS, **, NS v.s. AS) was calculated by t-test ($n=3$).

Rho-entrapped liposome was separated by gel filtration chromatography and added into PBS for dialysis. Outer solution was batched off at several time and the fluorescence intensity was measured by spectrofluorometer ($\text{Ex}=557 \text{ nm}$, $\text{Em}=577 \text{ nm}$). Leakage ratio was calculated from equation (1).

perature change and always showed the highest leakage value among the 3 models. This result indicates that changes in sphingoid content/species, even those that represent minor components in the model lipid compositions, are important factors for determining the permeability of the SC lipid model. In addition, the linear relationship between leakage and temperature indicates that there were no significant changes in the physicochemical conditions of the lipid membranes for the temperature range investigated. These results suggest that changes in the content of minor lipids due to the metabolic disturbance of ceramides caused by AD can affect membrane integrity (i.e., skin barrier function).

3.2 Physicochemical analyses

Figure 4 shows the scattering curve for the 3 models, as measured by SAXS. At 25°C, peaks indicating the lamellar structure were observed in all models, and no distinguishable differences in the SAXS pattern were found between the 3 model compositions. The results for the high q values at $q = 15.2$ and 16.9 nm^{-1} (0.37 nm and 0.41 nm, respectively) indicated that the lipid bilayer of all models formed organized orthorhombic lateral structures as part of a hydrated rigid gel state. J.A. Bouwstra *et al.* revealed that there are 3 packing structures for the lateral packing of a lipid bilayer: liquid crystal, hexagonal, and orthorhombic states, with the permeability dependent on the form of lateral packing¹⁸. In addition, the hydrated lipid bilayer composed of Cer 2/Chol/PA appeared to be very rigid, in good concordance with our 3 model lipids. **Figure 5** shows the SAXS patterns of NS after 1 h of incubation at each temperature. As the temperature increased, peaks indicating the lamellar structure and lateral packing tended to decrease.

Figure 6 shows the result of the fluorescent anisotropy measurements for the 3 hydrated model lipids during the

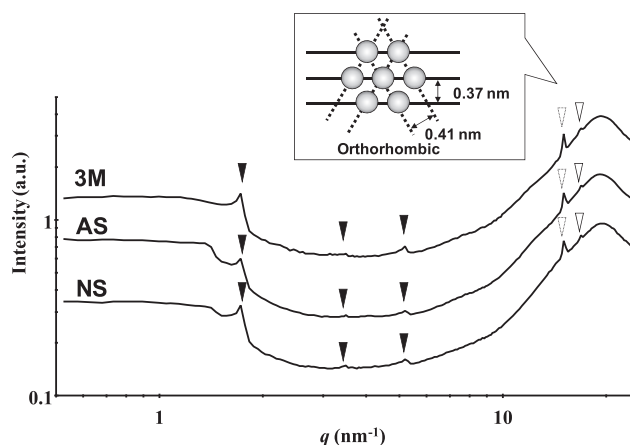


Fig. 4 SAXS data for comparison of three models. Lipid concentration was fixed at 100 mM for all samples. Measurement time was 1 h at 25 °C.

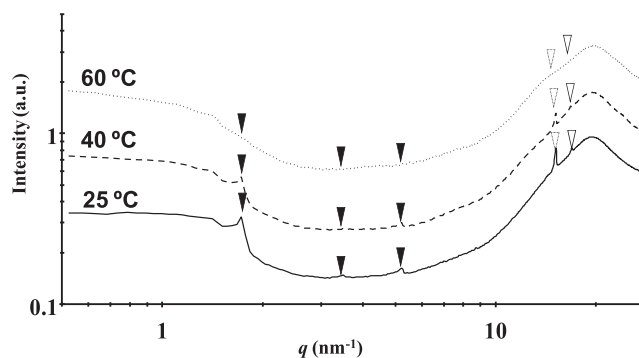


Fig. 5 SAXS data for comparison of temperature dependence for NS.

Lipid concentration was fixed at 100 mM for all samples. Samples were measured for 1 h after incubation at 25, 40 and 60 °C.

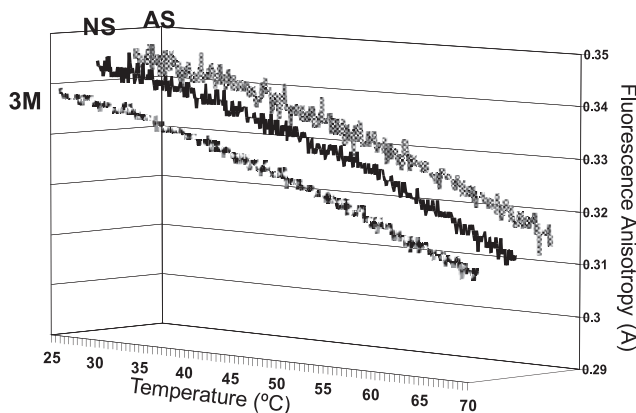


Fig. 6 Fluorescence anisotropy data.

Heating ratio was 1 °C/min and DPH was used as a fluorescence probe. Fluorescence intensity was measured by spectrofluorometer (Ex=351 nm, Em=430 nm). Fluorescence anisotropy (A) was calculated from equation (2). Lipid concentration was fixed at 10 mM for all samples.

heating process. Under a heating rate of 1 °C/min, no distinctive phase transition was observed. The intensity of the DPH anisotropy hardly changed for all models, indicating that the surrounding environment where the DPH was solubilized was in a relatively immobile condition¹⁹. In light of the disappearance of lateral packing at 60 °C after 1 h, as shown by SAXS, it is possible that packed lipids are annealing when the model lipids are exposed to a certain higher temperature for a certain period of time.

H. Watanabe *et al.* demonstrated that the phase diagram of Cer 5 (2-hydroxyacyl sphingosine)/Chol/PA (i.e., Cer 5/Chol/PA bilayer) was classified into 4 clusters, with no distinct phase transition temperature observed in cluster 3, as measured by fluorescence anisotropy²⁰. The liposomes

used in our present studies, consisting of Cer 2 (non-hydroxyacyl sphingosine)/Chol/PA at 12.5/34.5/53, correspond to cluster 3 in their phase diagram. Therefore, a distinct phase transition temperature was unlikely to be observed for our lipid composition, and a 1 °C/min heating rate resulted in an insufficient amount of time to carry out complete phase transition. Moreover, the physicochemical differences between the 3 types of liposomes, as assessed by fluorescent anisotropy and SAXS, were not evident (Fig. 4, 5 and 6).

In contrast to these physicochemical analyses, the leakage ratio of Rho encapsulated into the model liposomes differed significantly between the 3 models (Fig. 3). The leakage ratio for AS, a model of SC lipids for AD skin, was exceeded by NS and 3M throughout the temperature range of 25 °C to 60 °C. These results are consistent with our prior studies¹⁵) that showed an increase in released fluorescent dye from AS under anionic detergent stress. These results suggest that the permeability barrier function is influenced by the formation of local domains or clusters generated by alterations in the content and molecular species of sphingoid bases, which are minor constituents (less than 6% of the lipids). However, these local physicochemical changes appear to be undetectable by SAXS, which gives the phase conditions of the system as a whole within a sensitivity or resolution limit of each measurement. Therefore, if local and time-dependent formation of sphingolipid domains or clusters is the cause of barrier malfunction, we will not be able to distinguish them by using SAXS.

4 CONCLUSIONS

We investigated the effect of sphingoid bases on epidermal permeability barrier function. A significant difference was observed in the leakage ratio between model SC lipid liposomes with different sphingolipid ratios (So/Sa ratio of 5.43 for NS vs. 14.3 for AS[AD model]). Therefore, alterations in minor lipid composition in SC resulting from a ceramide metabolic abnormality can affect membrane integrity (i.e., the skin barrier function). However, neither SAXS nor fluorescence anisotropy measurements revealed physicochemical differences between 3M, NS, and AS. Hence, it is assumed that the altered lipid composition triggers local/transient membrane structural changes (i.e., the formation of domains or clusters). In comparison to other biological lipid membranes, intercellular lipid membranes in the SC have less flexibility and fluidity to prevent outflow of intercellular fluid. Therefore, local structural changes may affect epidermal barrier function, as observed in AD skin.

ACKNOWLEDGEMENT

We thank Prof. Kozo Takayama, Assis. Prof. Yasuko Obata and Mr. Hiroshi Watanabe (Department of Pharmaceutics, Hoshi University) for their assistance with the fluorescence anisotropy measurement and helpful discussions.

References

- 1) Elias, P. M.; Menon, G. K. Structural and lipid biochemical correlates of the epidermal permeability barrier. *Adv. Lipid Res.* **24**, 1-26 (1991)
- 2) Grayson, S.; Elias, P. M. Isolation and lipid biochemical characterization of stratum corneum membrane complexes. *J. Invest. Dermatol.* **78**, 128-135 (1982)
- 3) Holleran, W. M.; Takagi, Y.; Uchida, Y. Epidermal sphingolipids: metabolism, function and role(s) in skin disorders. *FEBS Lett.* **23**, 5456-5466 (2006)
- 4) Bouwstra, J. A.; Dubbelaar, F. E. R.; Gooris G. S.; Weerheim, A. M.; Poncet, M. The role of ceramide composition in the lipid organization of the skin barrier. *Biochim. Biophys. Acta* **1419**, 127-136 (1999)
- 5) tenGrotenhuis, E.; Demel, R. A.; Poncet, M.; Boer, D. R.; vanMiltenburg, J. C.; Bouwstra, J. A. Phase behavior of stratum corneum lipids in mixed Langmuir-Blodgett monolayers. *Biophys. J.* **71**, 1389-1399 (1996)
- 6) Downing, D. T.; Abraham, W.; Wegner, B. K.; Willman, K. W.; Marshall, J. L. Partition of sodium dodecyl sulfate into stratum corneum lipid liposomes. *Arch. Dermatol. Res.* **285**, 151-157 (1993)
- 7) Swartzendruber, D. C.; Wertz, P. W.; Kitko, D. J.; Madison, K. C.; Downing, D. T. Molecular models of the intercellular lipid lamellae in mammalian stratum corneum. *J. Invest. Dermatol.* **92**, 251-257 (1989)
- 8) Elias, P. M.; Brown, B. E.; Fritsch, P.; Goerke, J.; Gray, G. M.; White, R. J. Localization and composition of lipids in neonatal mouse stratum granulosum and stratum corneum. *J. Invest. Dermatol.* **73**, 339-348 (1979)
- 9) Elias, P. M.; Hatano, Y.; Williams, M. L. Basis for the barrier abnormality in atopic dermatitis: 'outside-inside-outside' pathogenic mechanisms. *J. Allergy Clin. Immunol.* **121**, 1337-1343 (2008)
- 10) Hatano, Y.; Man, M. Q.; Uchida, Y.; Crumrine, D.; Scharschmidt, T.; Kim E.; Mauro, T. M.; Feingold, K. R.; Elias, P. M.; Holleran, W. M. Maintenance of an acidic stratum corneum prevents emergence of murine atopic dermatitis. *J. Invest. Dermatol.* **129**, 1824-1835 (2009)
- 11) Nardo, A. D.; Wertz, P.; Giannetti, A.; Seidenari, S. Ceramide and cholesterol composition of the skin of patients with atopic dermatitis. *Acta Derm. Venereol.* **78**, 27-30 (1998)
- 12) Melnik, B.; Hollmann, J.; Hofmann, U.; Ynh, M.-S.; Plew, G. Lipid composition of outer stratum corneum and nails in atopic and control subjects. *Arch. Dermatol. Res.* **282**, 549-551 (1990)
- 13) Yamamoto, A.; Serizawa, S.; Ito, M.; Sato, Y. Stratum corneum lipid abnormalities in atopic dermatitis. *Arch. Dermatol. Res.* **283**, 219-223 (1991)
- 14) Man, M. Q.; Hatano, Y.; Lee, S. H.; Man, M.; Chang, S.; Feingold, K. R.; Leung, D. Y. M.; Holleran W.; Uchida, Y.; Elias, P. M. Characterization of a hapten-induced, murine model with multiple features of atopic dermatitis: structural, immunologic, and biochemical changes following single versus multiple oxazolone challenges. *J. Invest. Dermatol.* **128**, 79-86 (2008)
- 15) Loiseau, N.; Moradian, S.; Elias, P. M.; Holleran W. M.; Uchida, Y. *J. Invest. Dermatol.* **129**, S68 (2009).
- 16) Reiss, H. F.; Structure des phase liquide-cristalline de differents phospholipid vesicles. *Biochim. Biophys. Acta* **183**, 417-426 (1967)
- 17) Op den Kamp J. A.; Bonsen P. P. M.; van Deenen L. L. M.; Structural investigations on glucosaminyl phosphatidylglycerol from bacillus megaterium. *Biochim. Biophys. Acta* **176**, 298-305 (1969)
- 18) Boustra, J. A.; Gooris, G. S.; Salomons-de Vries, M. A.; von der Spek, J. A.; Bras, W. Structure of human stratum corneum as a function of temperature and hydration: a wide-angle X-ray diffraction study. *Int. J. Pharma.* **84**, 205-216 (1992)
- 19) Repakova, J.; Capkova P.; Holopainen, J. M.; Vattulainen, I. Distribution, orientation, and dynamics of DPH probes in DPPC bilayer. *J. Phys. Chem. B* **108**, 13438-13448 (2004)
- 20) Watanabe, H.; Obata, Y.; Onuki, Y.; Ishida, K.; Takayama, K. Novel preparation of intercellular lipid models of the stratum corneum containing stereoactive ceramide. *Chem. Pharm. Bull.* **58**, 312-317 (2010)